Materials Science & Engineering A 818 (2021) 141348

Contents lists available at ScienceDirect

Materials Science & Engineering A

journal homepage: www.elsevier.com/locate/msea

Effect of cold drawing strain on the microstructure, mechanical properties and electrical conductivity of low-oxygen copper wires

Fei Yang [a], Liming Dong [b], Lei Cai [c], Linfeng Wang [d], Zonghan Xie [e], Feng Fang [a,*]

[a] Jiangsu Key Laboratory of Advanced Metallic Materials, Southeast University, Nanjing, 211189, China
[b] School of Automotive Engineering, Changshu Institute of Technology, Changshu, 215500, China
[c] Sunnywell (China) New Material Technology Co. Ltd., Changzhou, 213200, China
[d] Technical Center of Baosteel Metal Co., Ltd, Shanghai, 200940, China
[e] School of Mechanical Engineering, University of Adelaide, SA, 5005, Australia

ARTICLE INFO

Keywords:
Cold drawing
Low-oxygen copper
Microstructure
Yield strength
Electrical conductivity

ABSTRACT

The effects of cold drawing process on the microstructure, mechanical properties and electrical conductivity of low-oxygen copper wires were studied. The results show that at low drawing strains ($\varepsilon \leq 1.23$), the plastic deformation is dominated by planar slip, some of grains are rotated along the drawing direction, giving rise to a <111> texture. At medium strains ($1.23 < \varepsilon \leq 1.91$), most of grains have re-oriented and laid parallel to the drawing direction, and the <111> and <100> textures are highly developed. At high strains ($\varepsilon > 1.91$), a fibrous structure is formed, with a staggered distribution of <111> and <100> textures. With the increase of drawing strain, the volume fraction of the <111> texture first increases and then decreases, while the volume fraction of the <100> texture increases monotonously. The yield strength first increases and then decreases, yielding the maximum value of 427.5 MPa at the strain of 1.91. Interestingly, the electrical conductivity of the copper wires changes with cold drawing strain and moves in the opposite way to the yield strength. The electrical conductivity first decreases and then increases with the minimum value at a strain of 1.91 (~87.5% IACS). At strains higher than 2.74, dynamic recrystallization occurs, resulting in a decrease in dislocation density and an increase in grain size. In addition to the dislocation density and grain size, the yield strength of the copper wires is further impacted by the texture development. The electrical conductivity is less influenced by dislocations and vacancies. Instead, it is dominated by those grain boundaries perpendicular to the drawing direction. An excellent strength-conductivity combination was achieved by tailoring the microstructure of copper wires. For example, a wire with the yield strength (YS) of 400.5 MPa and electrical conductivity (EC) of 94.3% IACS was acquired when the drawing strain reaches 2.74.

1. Introduction

Low-oxygen copper wires are extensively used as electrical conductors in a variety of electric and electronic applications [1]. As the two most important properties, the mechanical strength and electrical conductivity are mutually exclusive and hard to raise up simultaneously [2]. Consider this. It is essential to improve the strength of copper wires through work hardening process. However, the defects induced by deformation would cause damage to electrical conductivity [3], because defects will lead to electron scattering and increased resistivity. Matthiessen et al. believed that the electrical resistivity is regulated by two factors [4,5]: one is the thermal effect, which is proportional to the ambient temperature; while the other is the internal defects, which is mainly related to the microstructure, including dislocations, vacancies, grain boundaries (GBS), precipitates and solute atoms. Therefore, the crystal defects caused by work hardening have a positive effect on the strength but reduce electrical conductivity [6]. Overcoming a trade-off between the strength and electrical conductivity has become a major challenge in the manufacture of copper wires with high performance [7].

The effects of different deformation methods on the hardness and electrical conductivity of copper alloys have been studied [8]. It is believed that the ultrafine grain structure (grain size within 100 nm) produced by severe plastic deformation can greatly improve the strength while maintaining good plasticity and electrical conductivity. The tensile strength and yield strength of copper wire, obtained by

* Corresponding author. School of Materials Science and Engineering, Southeast University, Jiangning District, Nanjing, 211189, China.
E-mail address: fangfeng@seu.edu.cn (F. Fang).

https://doi.org/10.1016/j.msea.2021.141348
Received 9 March 2021; Received in revised form 13 April 2021; Accepted 20 April 2021
Available online 4 May 2021

equal-channel angular hydro-extrusion, direct hydro-extrusion and drawing processing, are 686 MPa and 10% respectively [9]. And the effect of heat treatment on the behaviour of the elastic characteristics has been investigated [10]. The drawing process of pure copper obtained from powder metallurgy was also studied [11]. Apart from the interference of thermal factors, the resistivity is only regulated by the interaction of electrons and defects. Similarly, the microstructure of cold-drawn aluminium wire was researched [12], and the results showed that the grain morphology, deformation texture and precipitation of the second nanoscale phase all led to changes in electrical conductivity. For drawing copper wire [13], a large number of dislocations were produced in the microstructure after severe deformation; the original grains were greatly refined, and a fibrous structure was formed. With increasing drawing strain, the grain refinement and dislocation proliferation caused by plastic deformation were more obvious, and the tensile strength of copper wire increased from 230 MPa to 460 MPa and maintained a conductivity of 96.5% IACS. Regarding pure metal, defects have a critical effect on electrical conductivity [14]. Cold drawing deformation is a generic method to prepare copper wires, and leads to variations in dislocations, grain boundaries, vacancies and textures [15–17]. However, which structure is beneficial to strength and conductivity has yet to be determined [18,19]. Moreover, analysis of the relationship between the microstructure and strength is scarce, especially the influencing factors of conductivity, and has become an urgent problem to be resolved [20].

In this work, the microstructure of copper wire at different drawing strains is detected. The effects of grain boundaries, dislocations and textures on the strength and conductivity are determined by introducing a strengthening mechanism and electron scattering model. Then, theoretical guidance for the preparation of high-performance ultrafine copper wires with both strength and conductivity is provided.

2. Materials and methods

Commercial continuous-casted and rolled pure copper rods with diameters of 8 mm were selected as the raw material. The chemical composition is given in Table 1. To eliminate the influence of temperature caused by friction between the copper rod and die, the drawing speed was set to a low value of 1 m/min. After each step, the wire was air cooled until the temperature of the wire decreased to room temperature, and then the next drawing test was conducted. After 18 drawing passes, a copper wire with a maximum deformation of 96.9%, cumulative strain of 3.47 and diameter of 1.41 mm was obtained. The microstructure was observed by field-emission scanning electron microscopy (SEM) on a Sirion-400 microscope. Electron backscatter diffraction (EBSD) was used to detect the microstructure and crystallographic orientation, and the data were processed by Channel 5 software. Transmission electron microscopy (TEM, JSM-2100F) was utilized to observe the dislocation configuration. The tensile mechanical properties were tested on a CMT5105 electronic universal testing machine. A cylindrical sample with a length of 150 mm was used, and the tensile rate was $5 \times 10^{-3}\ s^{-1}$ at room temperature. Three groups of tensile tests were carried out for each sample. The conductivity of the sample was measured by a QJ57 DC double-arm bridge. The length of the test sample was 500 mm. To eliminate the influence of the environment, the room temperature was kept at 20 °C. The electrical conductivity of the material is expressed by the International Annealed Copper Standard (IACS), and the calculation formula is as follows:

$$w(\%IACS) = L/(R.S \times 5.8 \times 10\hat{7}) \times 100\%$$

Table 1
Composition of the low-oxygen copper (wt%).

Element	O	Impurity	Cu
Content/%	0.02–0.04	0.0065	Bal.

where L is the length of the specimen, R is the resistance of the specimen, and S is the cross-sectional area of the specimen.

3. Results

3.1. Microstructural evolution

Microstructure of copper wires with different drawing strains is shown in Fig. 1. The grain boundary of the original wire is straight and clear, and there are many twins in the grains, as shown in Fig. 1a. According to reports, the stacking fault energy of pure copper is 35–40 mJ m^{-2} [21,22]. Owing to the short time, high speed and high temperature of hot deformation, a large number of annealing twins are produced in the grains. As the drawing strain increases, the grains are flattened and elongated, and the grain boundaries are prone to rotate parallel to the drawing direction. The annealing twins are destroyed, and the deformation is dominated by dislocation slip. In this situation, the deformation is uneven because the partial slip system of the crystal is not activated. The grains are mainly strip-shaped and inclined to the drawing direction, but a few grains still maintain an equiaxed structure, as shown in the yellow box of Fig. 1b. When the drawing strain reaches 1.91 (Fig. 1c), the slip system of the crystal is fully activated, and the grain boundaries are almost parallel to the drawing direction. With an increasing drawing strain, the lamellar spacing decreases continuously, and the microstructure has no obvious change (Fig. 1d).

Fig. 2 shows the TEM morphology of the copper wires. Compared with the original sample (Fig. 2a), after drawing at 0.58 strain, the dislocation density increases significantly. A large number of dislocations are entangled in the grain, and the accumulation of dislocation group leads to a local dislocation density surge, showing dislocation walls and dislocation substructures (Fig. 2b). Hughes [23] classified these layered boundaries as geometrically necessary boundaries. That are necessary for adapting to the lattice rotation caused by slip in adjacent volumes. Sub-grains are formed in the elongated grains due to the accumulation of dislocations, accompanied by the elongation and splitting of grains. When the strain reaches 1.91 (Fig. 2c), a large number of elongated grains with width of 100–200 nm are found. The dislocation density in the microstructure increases continuously and evolves to dislocation cells. The cell wall is composed of dislocations, but the dislocation density inside the cell is dispersed.

At high strain (Fig. 2d), a strip structure is formed in the grains along the axial direction of drawing. The dislocation walls and low-angle grain boundaries are gradually transformed into high-angle grain boundaries due to the slip and accumulation of dislocations. A certain amount of recrystallized grain is observed, as shown in Fig. 2e. On the one hand, the recrystallization temperature of pure copper is low, approximately 170 °C [24], and drawing will produce high thermal isolation stress, resulting in continuous dynamic recrystallization. Continuous dynamic recrystallization is the process of continuously absorbing dislocations in the sub-grain boundaries during thermal deformation [25]. On the other hand, the deformation storage energy increases with the increasing number of drawing passes, promoting the frequency of recrystallization, as shown in Fig. 2f.

Fig. 3 shows the grain orientation of the copper wire, and the upper right corner of Fig. 3a is the colour orientation mark. The orientation of grains in the original structure is random. The average grain size including twin boundaries is approximately 7.3 μm, as measured in accordance with the line intercept method. At a strain of 0.58, the grains are extruded along the drawing direction (Fig. 3b). The colour gradient inside the grain represents the misorientation caused by the non-uniform torsion deformation, and a shallow <111> texture emerges. When the drawing strain reaches 1.23 (Fig. 3c), the grains are severely deformed, and a <100> texture largely develops. The grains are completely transformed into <111> and <100> orientations after the strain increases to 1.91 (Fig. 3d). At the same time, it is observed that the

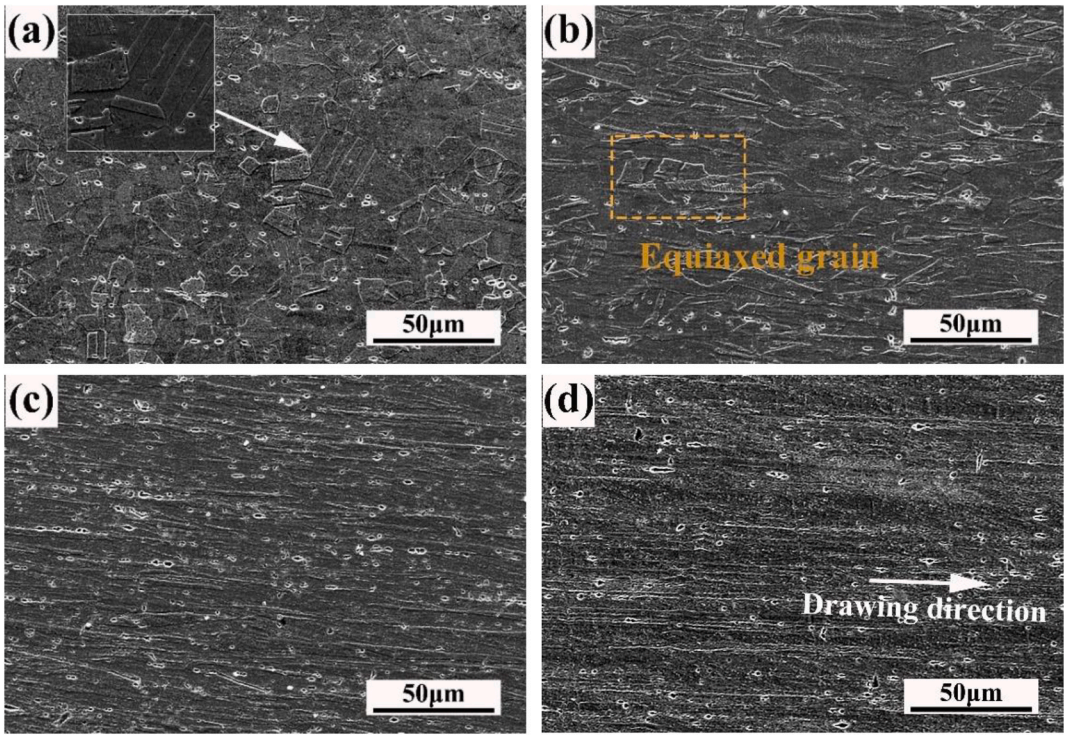

Fig. 1. Microstructure of the longitudinal section with (a) undeformed ε = 0, (b) ε = 0.58, (c) ε = 1.91, and (d) ε = 3.47.

grains are clearly broken. With a further increase in the drawing strain, the grains are continuously refined, and the fibre structure with <111> and <100> textures is characterized (Fig. 3e and f).

The degree of deformation of grains with different orientations is also different. Regarding materials with high fault energy, such as pure copper, plastic deformation is mainly dominated by sliding [26–28]. Grains with distinct orientations are subjected to different external forces. At high drawing strains, the uniformity of deformation largely improves. Fig. 4 shows the kernel average misorientation (KAM) of copper wires at different drawing strains, and the colour gradient represents the magnitude of the local strain. The results demonstrate that the higher the drawing strain is, the strain is more distributed in the structure. This result suggests that the deformation between adjacent grains is further coordinated.

The volume fraction of the high- and low-angle grain boundaries (HAGBs and LAGBs, respectively) was obtained by orientation image microscopy (OIM) software, and the results are shown in Fig. 5. In addition, the misorientation of boundaries less than 2° are excluded in the statistical scope. The proportion of grain boundaries is calculated as following [29,30]:

$$V_{HAGB} = \frac{N_{HAGB}}{N_{HABG} + N_{LAGB}} \tag{1}$$

where V_{HAGB} is the volume fraction of the HAGBs, N_{HAGB} is the sum of the number of HAGBs, and N_{LAGB} is the sum of the number of grain boundaries between 2 and 15°. In the original copper sample, HAGBs account for 97.1% of the grain boundaries, resulting from the dynamic recovery or recrystallization produced by hot deformation. After drawing from 8 mm to 6 mm (ε = 0.58), the fraction of LAGBs increases rapidly, to approximately 76.6%, and V_{HAGB} clearly decreases compared with that without deformation. Plastic deformation leads to torsion and fragmentation of the original large grains. At the same time, a large number of dislocations are generated by the activation of the slip system. The dislocation tangles that form substructures, such as dislocation cells, will lead to an increase in the number of sub-grain boundaries.

When the strain reaches 1.23, the grain boundaries are dominated by LAGBs. As mentioned above, the grains are elongated along the drawing direction, the macro-texture reduces the misorientation between grains, and the HAGB is gradually replaced by the LAGB. At the same time, the grains are broken during the deformation process. The structure of the grain boundaries becomes more complicated, and the number of sub-grain boundaries increases. With the accumulation of drawing strain, the proportion of LAGBs no longer increases and instead shows a continuous downward trend. When the strain is 3.47, the proportion of small-angle grain boundaries continues to decrease to 38.8%. Correspondingly, the proportion of HAGBs increases steadily, which is related to dynamic recrystallization.

3.2. Mechanical properties

The tensile test was carried out at room temperature, and the engineering stress-strain curve is shown in Fig. 6a. The tensile yield strength and elongation versus drawing strain are shown in Fig. 6b. It can be seen that with an increasing drawing strain, the yield strength of the copper wire first increases and then decreases slightly. The strain ε = 1.91 reaches the maximum value of 427.5 MPa, 3 times higher than that of the undeformed sample. The decrease in strength may be related to dynamic recrystallization. However, the elongation presents a monotonically decreasing trend, indicating that work hardening causes considerable damage to the plasticity of the copper wire.

3.3. Electrical conductivity

Electrical conductivity was tested, and the results are presented in Fig. 7. The conductivity of the undeformed (ε = 0) copper rod is 97% IACS. When the strain is lower than 1.91, the conductivity of the copper wire decreases with an increasing drawing strain and reaches the lowest value of 87.5% IACS at a strain ε = 1.91, which is 9.5% lower than that of the original sample. When the strain is higher than 1.91, the conductivity begins to increase. In contrast to the change in strength, with increasing drawing strain, the conductivity of copper wire first decreases and then increases. Fig. 2 shows the dislocation propagation and slip as

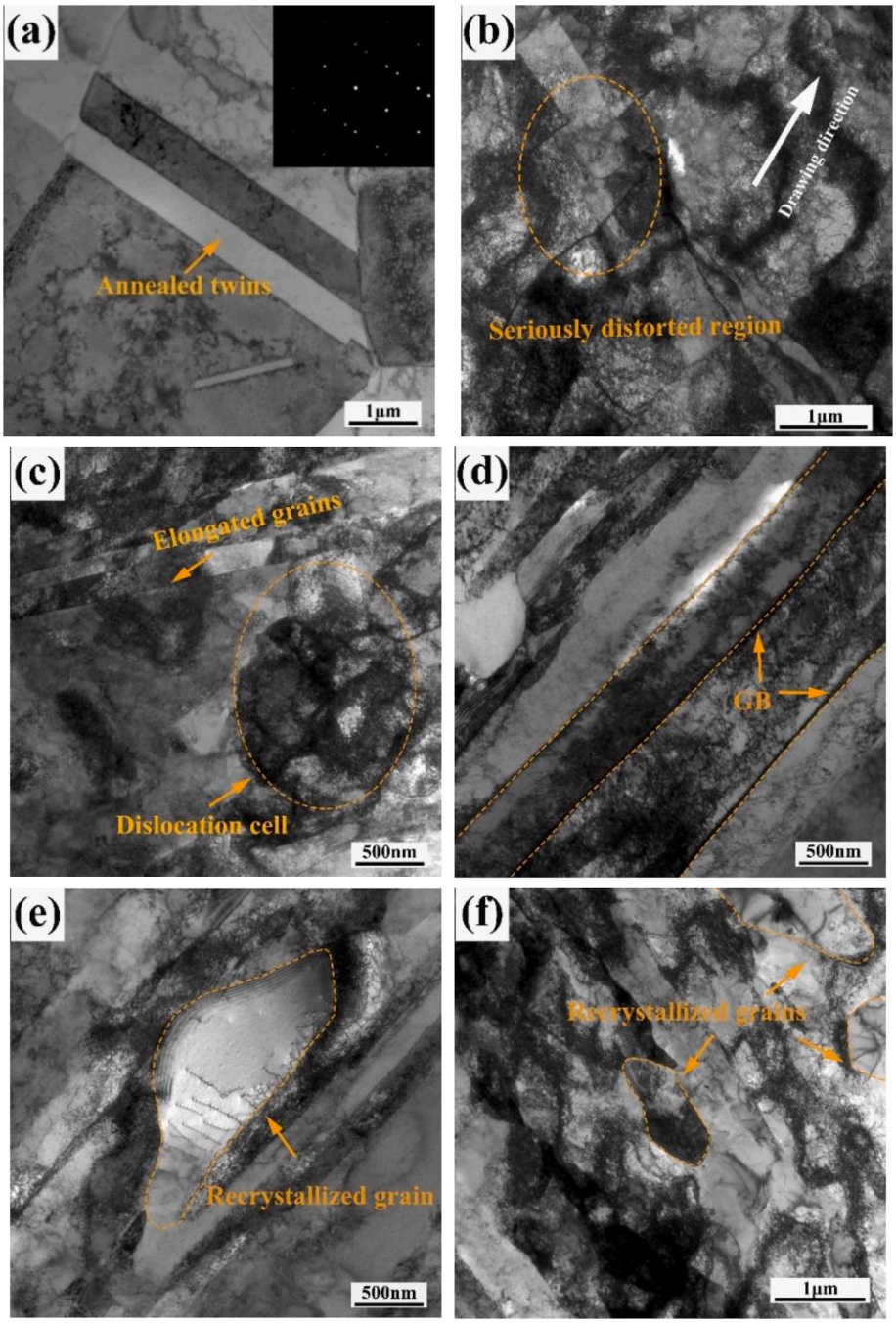

Fig. 2. TEM bright field images at strains of (a) undeformed, (b) $\varepsilon = 0.58$, (c) $\varepsilon = 1.91$, (d, e) $\varepsilon = 2.74$, and (f) $\varepsilon = 3.47$.

well as grain fragmentation and elongation. It is preliminarily speculated that a large number of defects caused by deformation hinder the transmission of electrons, resulting in the decrease in electrical conductivity. However, when the cumulative drawing strain is larger than 1.91, the copper wire recrystallizes. The dislocation density in the recrystallized grains decreases, and the microstructure becomes more uniform, so the electrical conductivity of the copper wire recovers.

4. Discussion

4.1. Influencing factors of strength

During the drawing process, the grain is elongated and refined, and the proliferation of dislocations and dynamic recrystallization occur. Regarding high-purity low-oxygen copper wire, the variation in strength is based on the combination of grain boundary strengthening and dislocation strengthening. Thus, the strength calculation is as follows [31]:

$$\sigma_{0.2} = \sigma_0 + \sigma_{GB} + \sigma_{DIS} \tag{2}$$

where $\sigma_{0.2}$ is the tensile yield strength and σ_0 is the lattice friction stress. The magnitude of the friction stress is significantly affected by the orientation factor, and for pure copper, it is 25 MPa [32]. Moreover, σ_{GB} is the grain boundary strengthening brought about by refinement, and σ_{DIS} is the work hardening caused by dislocation propagation. The grain boundary strengthening can be evaluated by the Hall-Petch formula [33]:

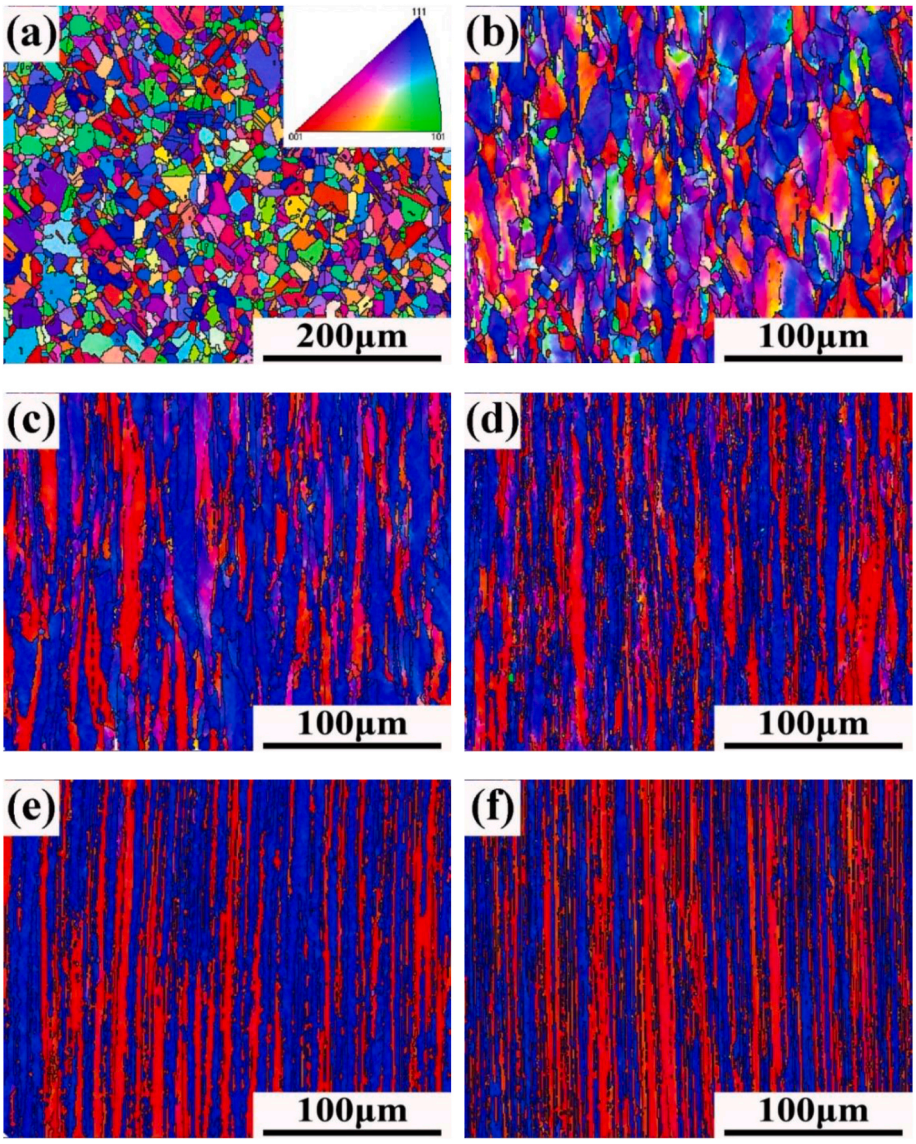

Fig. 3. IPF images in the drawn direction at strains of (a) undeformed, (b) ε = 0.58, (c) ε = 1.23, (d) ε = 1.91, (e) ε = 2.74, and (f) ε = 3.47.

$$\sigma_{GB} = Kd^{-1/2} = 110 \cdot d^{-1/2} \quad (3)$$

where K is the Hall-Petch constant, which is 0.11 MPa m^{-2} for pure copper [34], and d is the average grain size. It should be pointed out that the Hall-Petch slope depends on the GB structure. Compared with general GBs, special GBs have higher K values. In the cold-drawn copper wire, the effective grain size is estimated to be twice the width of the lamellar structure because most of the grains are elongated along the drawing direction [12].

The contribution of dislocation strengthening is calculated by the Taylor formula [35]:

$$\sigma_{DIS} = \alpha M G b \rho^{\frac{1}{2}} \quad (4)$$

$$\rho = 14.4\varepsilon^2 / b^2 \quad (5)$$

where α is a constant because FCC materials is usually taken as 0.24 [36]; M stands for the Taylor factor of 3.06; G is the shear modulus, 45.6 GPa [37]; B is the Burgers vector, $\frac{\sqrt{2}}{2}a = 0.256\ nm$ [38]; ρ is the dislocation density; and ε is the micro-strain measured by XRD [35]. The σ_{GB} and σ_{DIS} results from the calculation are shown in Table 2.

As predicted, the yield strength is mainly affected by grain boundaries and dislocations. At the beginning of deformation, the grain size decreases continuously because of the elongation and fragmentation of the grains. At a strain of 3.47, the grain size increases slightly as a result of dynamic recrystallization. The dislocation density first increases and then decreases, and thermal insulation stress leads to the dynamic recovery of dislocations. As shown in Fig. 2e and f, the dislocation density in the recrystallized grain is low.

Table 2 illustrates that there is a difference between theoretical and actual yield strength. In addition to the dominant role of dislocations and grain boundaries, there are other factors affecting strength. From the IPF diagram in Fig. 3, it can be found that there are two kinds of fibre textures in the cold-drawn copper wires, namely, <001> and <111>. The Schmidt factors of the <001> and <111> orientations measured by channel 5 are in the ranges of 0.42–0.46 and 0.3–0.34, respectively. According to Schmidt's law, the Schmidt factor of a single crystal orientation is inversely proportional to its yield strength; that is, the smaller the Schmidt factor is, the greater the yield strength. Therefore, the yield strength of <111>-oriented grains is greater than that of <001>-oriented grains. Compared with the <001> texture, the <111> texture can be called a hard orientation. To quantitatively analyse the changes in the <111> and <001> fibre textures, their volume fractions are calculated by the following formula [39]:

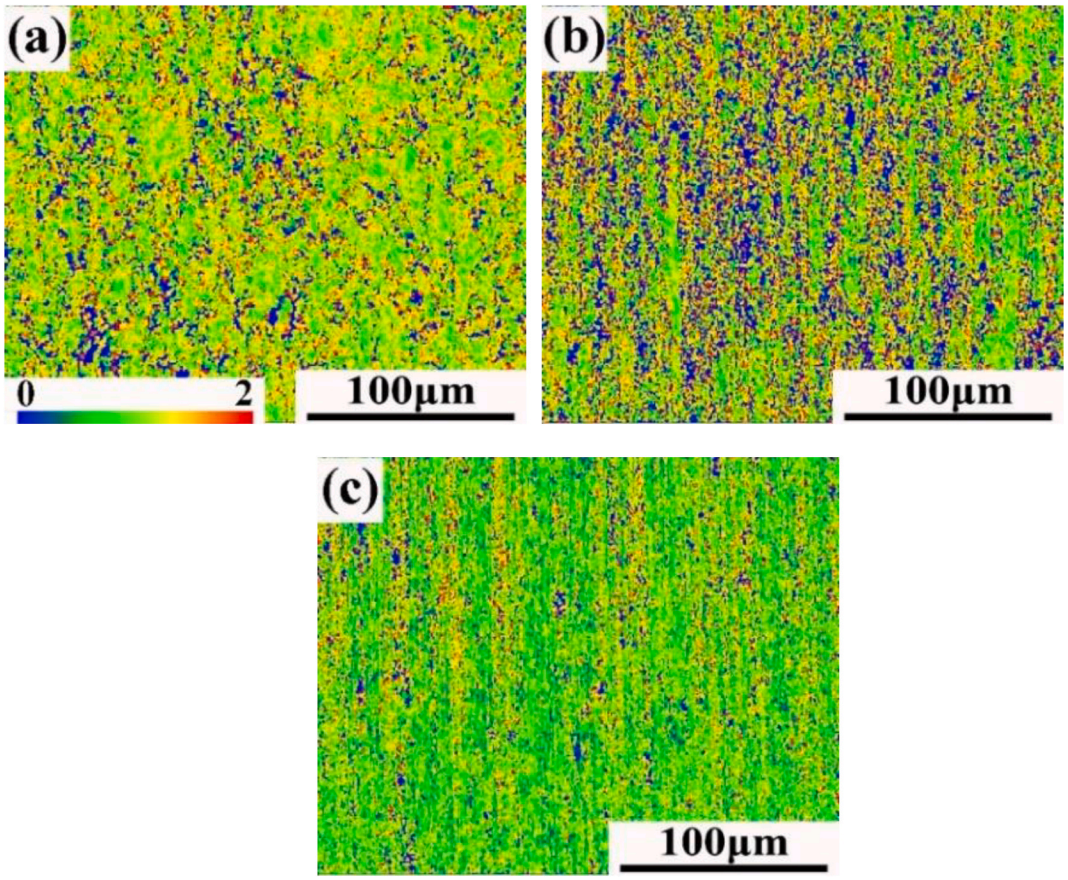

Fig. 4. Kernel average misorientation at strains of (a) ε = 0.58, (b) ε = 1.91, and (c) ε = 3.47.

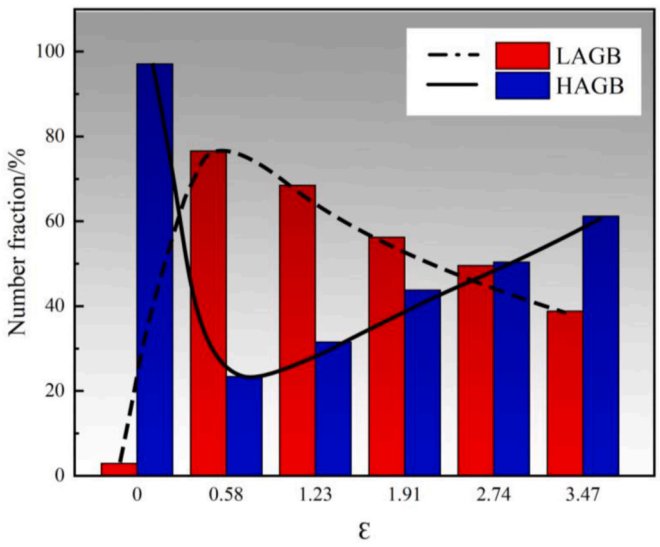

Fig. 5. Misorientation angle variation of cold-drawn copper wires.

$$f_{<HKL>} = \frac{S_{<HKL>}}{S} \tag{6}$$

where $f_{<HKL>}$ represents the volume fraction of the <HKL> texture, $S_{<HKL>}$ is the area of the grains with the <HKL> texture, and S represents the total area of the statistical area. The statistical results are presented in Fig. 8. When the strain is lower than 1.23, the volume fraction of the <111> texture increases rapidly with increasing strain, from an initial 32.7%–62.3%; when the drawing strain increases to 1.91, the <111> texture grows slowly, and there is a slight decrease in the subsequent drawing process. However, the volume fraction of the <100> texture increases continuously with an increasing drawing strain.

It is common knowledge that the sliding direction of crystal grains with the <111> orientation is symmetrically distributed with respect to the axial direction and is beneficial to maintain the circular cross-section of the wire during the cold drawing process [40]. Therefore, a stable <111> texture will eventually be formed in the face-centred cubic metal during the drawing deformation. However, the formation mechanism of the <100> texture in FCC metals is controversial. Jetter et al. [41] considered the effect of temperature on the fibre texture and considered that the <100> texture was caused by recrystallization and twinning. Chen Jian et al. [39] believed that the stability of <100> fiber texture is due to the change of the slip mechanism from planar slip to wavy slip. In this work, the volume fraction of the <100> fibre texture increased continuously with an increasing drawing strain, which may also be influenced by the activation of cross slip.

It can be seen from Fig. 8 that the fraction of the <111> texture is saturated at a strain of 1.91 and no longer increases. Therefore, when the drawing strain continues to increase, the <111> texture provides no contribution to the increase in tensile strength. This result is consistent with the change trend of $\Delta\sigma_{0.2}$in Table 2. The results demonstrate that the strength of cold-drawn copper wire is not only related to grain refinement and dislocation propagation but also affected by the texture components.

4.2. *Influencing factors of electrical conductivity*

According to the Matthiessen criterion, the resistance coefficient (Ω) of metal materials is mainly affected by intrinsic properties, grain

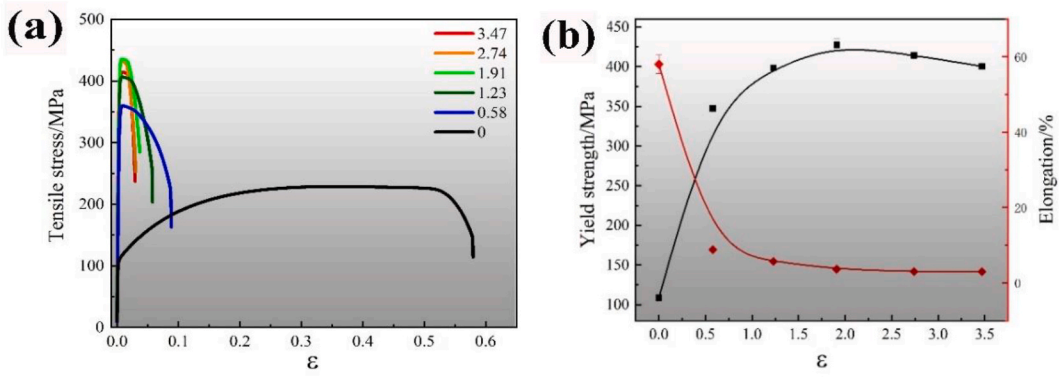

Fig. 6. (a) Engineering stress-strain curves and (b) yield strength and elongation versus drawing strain.

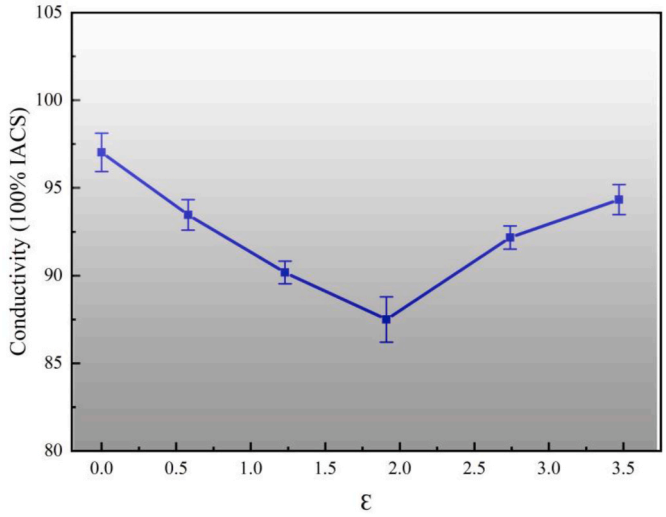

Fig. 7. Conductivity of low-oxygen copper at different strains.

boundaries, dislocations, vacancies and precipitates [5,42]. For drawing copper wire at room temperature, the resistance coefficient can be expressed as follows [43]:

$$\Omega = \Omega_{Cu} + \Omega_{Gb} + \Omega_{Dis} + \Omega_{Vac} \tag{7}$$

where Ω_{Cu} is the resistivity of the defect-free pure copper at room temperature, 1.724×10^{-8} Ω·m [20]; and Ω_{GB}, Ω_{Dis}, and Ω_{Vac} represent the scattering effects of the grain boundaries, dislocations, and vacancies, respectively. Formula (7) can be modified as follows [12,19]:

$$\Omega = \Omega_{Cu} + S_{Gb}\,\Delta\Omega_{Gb} + \rho_{Dis}\Delta\Omega_{Dis} + C_v\Delta\Omega_{Vac} \tag{8}$$

Among them, the influence of the unit density of grain boundaries $\Delta\Omega_{GB}$, dislocations $\Delta\Omega_{Dis}$, and vacancies $\Delta\Omega_{Vac}$ on the resistivity has been widely reported, having values of 2.2×10^{-16} Ωm^2, 2.0×10^{-25} Ωm^3, 2.6×10^{-8} Ωm/at.%, respectively [20,44,45]. Moreover, S_{Gb} is the proportion of grain boundaries per unit volume, ρ_{Dis} is the dislocation density, and C_v is the vacancy concentration. According to previous reports, ρ_{Dis} of the drawn copper wire is generally lower than 7×10^{14} m^{-2} [42]. The vacancy concentration C_v of the severely plastic-deformed metal material is approximately 10^{-3} at.% [46]. This value is calculated from the increase in resistivity due to dislocations and vacancies, which are 1.4×10^{-10} Ω·m and 2.6×10^{-11} Ω·m, respectively, and much lower than the intrinsic resistivity of pure copper (1.724×10^{-8} Ω·m). The influence of dislocations and vacancies on the resistivity of the drawn copper wire is almost negligible. J.P. Hou [12] concluded that the electrical resistivity of pure aluminium wire with severe plastic deformation is mainly affected by the volume fraction of the grain boundary.

Fig. 9 shows the distribution of HAGBs, and the grain size of copper wires is counted (grain boundary angle greater than 15°). The results are listed in Table 3. There are a large number of annealing twins in the initial copper rods. Han K et al. [18]. Believed that the twins would relax the grain boundaries and could cause a significant decrease in resistivity, so they were not within the scope of these statistics. It can be seen from Table 3 that with an increasing drawing strain, the aspect ratio of grains increases continuously, and the original equiaxed grains change into strip structures. The grain size parallel to the drawing (axial) direction decreases first and then increases. In the process of drawing, the grains suffer axial tension and transverse pressure. At the beginning of drawing, the grains are elongated and seriously broken. The broken grains produce more grain boundaries, resulting in a continuous decrease in the axial grain length. Although the size of these broken grains is small, the distribution is relatively concentrated, and the effect of electron scattering is obvious. When the strain is greater than 1.91, the grains are almost parallel to the drawing axis, the rotation and fragmentation of grains are reduced, and the size difference between grains is fuzzy. Compared with Fig. 9c, the number of small grains decreases significantly in Fig. 9d; thus, the effect of grain boundaries on resistivity is weakened. In the drawn copper wire, there are some seriously elongated grains, whose axial length is hundreds of microns. It can be seen from the corresponding texture orientation in Fig. 3 that the seriously elongated grains are generally <100> oriented. Considering the low Schmidt

Table 2
Strength contributions of the grain boundaries and dislocations.

ε	d	σ_{GB}/MPa	ρ/m^{-2}	σ_{Dis}/MPa	The.$\sigma_{0.2}$	Mea.$\sigma_{0.2}$	$\Delta\sigma_{0.2}$
0	7.29 μm	40.7	2.1×10^{13}	39.3	105.0	107.5	2.5
0.58	756 nm	126.5	4.2×10^{14}	181.4	332.9	346.4	13.5
1.23	607 nm	141.2	5.4×10^{14}	201.1	367.3	396.6	29.3
1.91	495 nm	156.3	6.3×10^{14}	215.1	396.4	427.5	31.1
2.74	451 nm	163.8	5.8×10^{14}	206.4	395.2	414.5	19.3
3.47	472 nm	160.1	5.3×10^{14}	197.3	382.4	400.5	18.1

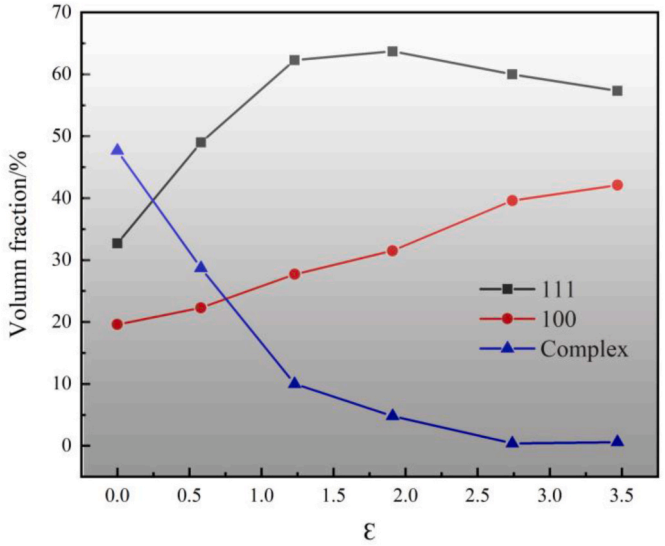

Fig. 8. Variation in the texture components as a function of strain.

factor of <100> oriented grains, these dislocations are more likely to slip, so they have higher plastic deformation ability in the drawing process, and their probability of fragmentation is smaller than that of <111>-oriented grains.

A schematic diagram of the scattering effect of deformed structure on electrons is shown in Fig. 10. There are two types of grain boundaries in drawn copper wires, namely, GB_P parallel to the drawing direction and GB_V perpendicular to the drawing direction. Since the current direction is parallel to the drawing axis, the two types of grain boundaries contribute differently to resistivity. Generally, the increase in resistivity caused by GB_V should be much greater than that of GB_P. Therefore, the frequency of electron scattering is high as the spacing between GB_Vs is small. The GB_V frequency per unit length (F_{GBv}) can be used to characterize the effect of grain boundaries on electrical resistance (R).

$$F_{GBv} = \frac{L}{d_{GB_v}} \tag{9}$$

where L is the unit length (m) and $d_{GBv}$is the average spacing between GB_V. The variation in GB_V is combined with that of resistivity, as shown in Fig. 11. The changes in GB_V and resistivity are almost consistent, also confirms that the conductivity of copper wire is closely related to GB_V. It can be deducted that the F_{GBv} is inversely proportional to d(GB_V) and proportional to R. The reduction of small-sized grains at a high drawing strain leads to an increase in the average axial grain size, as showed in Fig. 9. At the same time, a large number of recrystallized grains are formed. Fig. 12 shows the distribution of recrystallization at a strain of 3.47. Dynamic recrystallization is prone to occur in grain boundaries and sub-grains. However, the grain size is smaller, and its longitudinal length is shorter than 1 μm (as shown in Fig. 2f), which has a negative effect on conductivity.

It is found that GBs have a significant effect on the strength and

Table 3
Statistics of grain size in the axial and transverse directions.

Grain size/ μm	$\varepsilon = 0$	$\varepsilon =$ 0.58	$\varepsilon =$ 1.23	$\varepsilon =$ 1.91	$\varepsilon =$ 2.74	$\varepsilon =$ 3.47
Axial	13.7	8.7	7.9	5.4	6.6	6.2
Transverse	12.2	4.3	2.9	2.3	1.9	1.4
Aspect ratio	1.1	2.0	2.7	2.3	3.5	4.4

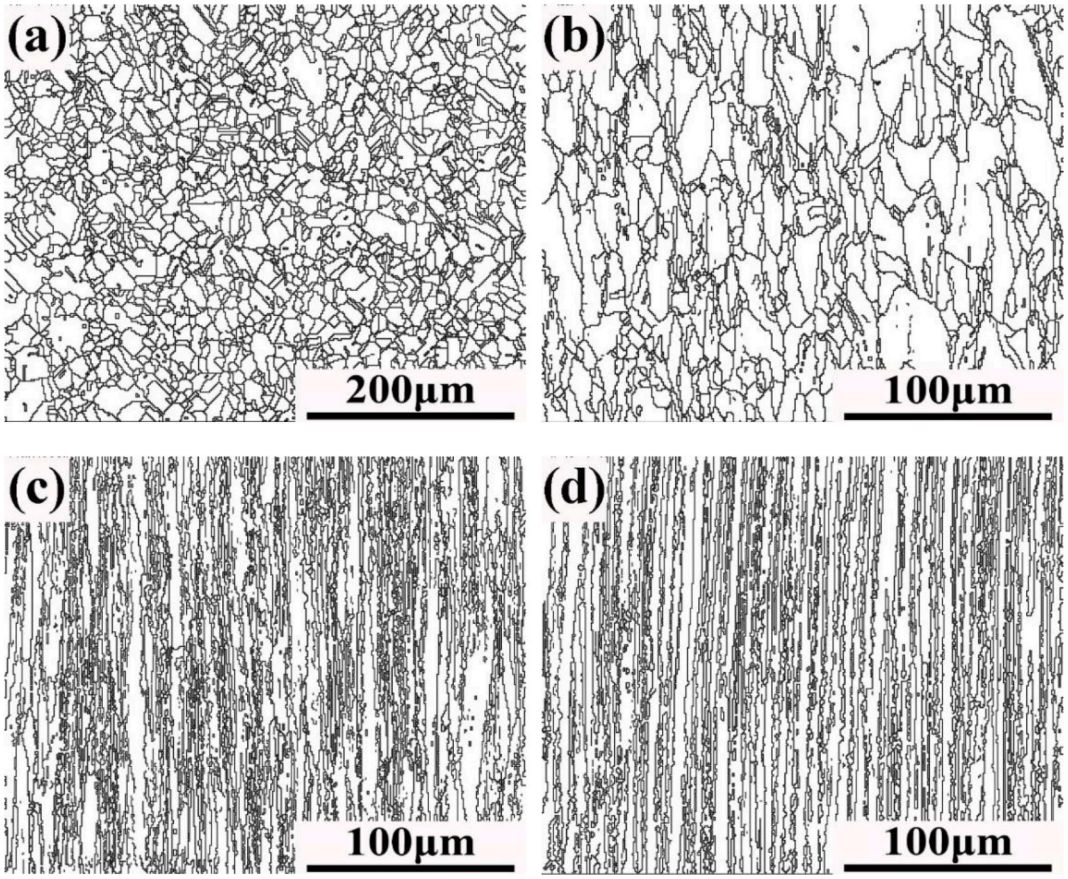

Fig. 9. Distribution of high-angle grain boundaries: (a) undeformed, (b) ε = 0.58, (c) ε = 1.91, and (d) ε = 2.74.

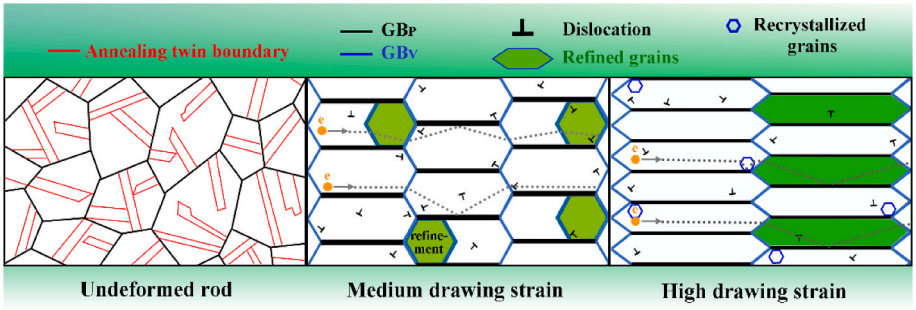

Fig. 10. Schematic diagram of electron scattering by deformed structure.

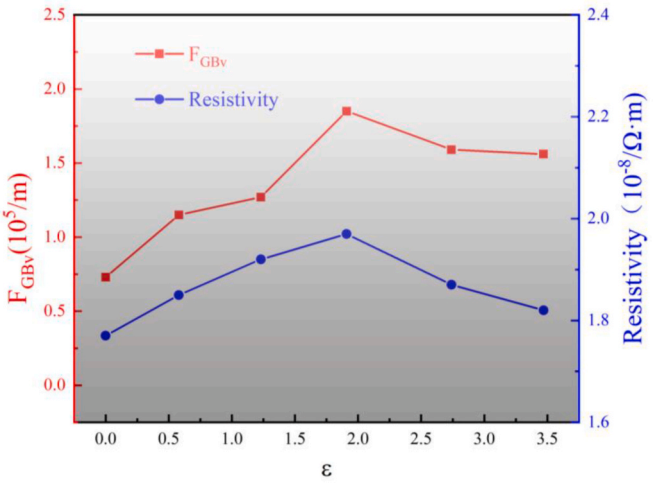

Fig. 11. and resistivity versus drawing strain.

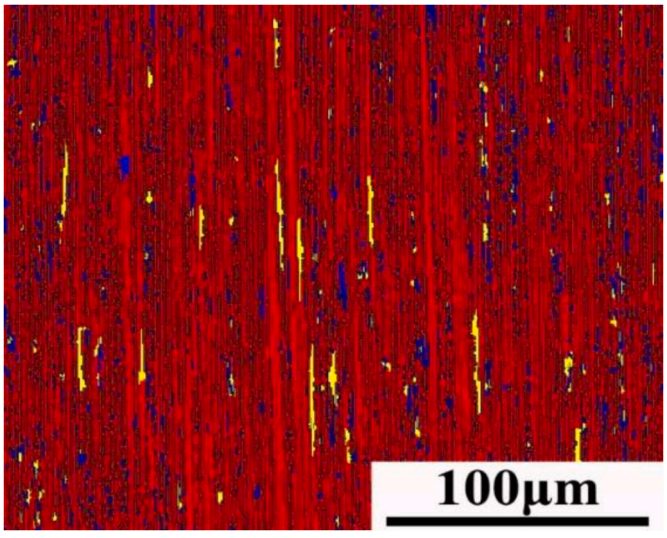

Fig. 12. Recrystallization of copper wire at ε = 3.47.

conductivity of the copper wire. With the increase of drawing strain, the continuous decrease in spacing between GB_P reduces the mean free path of dislocation movement and improves the work hardening of the material [47]. The scattering of electrons is mainly determined by GB_V, and the GB_P plays a large role in strength. Therefore, through reasonable control of the grain morphology, increase GB_P and decrease GB_V, copper wire with an elongated and uniform microstructure can be obtained. Fig. 13 revels the relationship between drawing strain, yield strength and electrical conduction. At a strain of 2.74, a yield strength of 400.5 MPa can be achieved along with a conductivity of 94.3 IACS. Compared with the original sample, the strength is increased by 273%, and the electrical conductivity is hardly affected.

For drawing copper wire, the evolution of microstructure is mainly related to dislocation and grain boundary. The electron scattering effect of dislocations is much lower than that of grain boundaries. The grain boundary can be divided into GB_V and GB_P. GB_P has little effect on electron scattering because it is parallel to the drawing direction. According to the Hall-Petch formula, with the reduce of distance between GB_Ps, the average free path of dislocation motion also decreases, which leads to the significant effect of grain refinement strengthening. GB_V has a greater impact on conductivity, and an increase in GB_V spacing will reduce the frequency of electron scattering. In summary, to obtain high-performance copper wire, spacing between GB_Vs should be increased as much as possible, while spacing between GB_Ps should be reduced. It is necessary to increase the drawing strain of the cooper wire to obtain elongated fibrous grains. In addition, drawing at a low temperature can inhibit the recrystallization of the fibrous grain. Therefore, it will be good for reduce the scattering effect of newly formed grain boundaries.

5. Conclusions

The mechanical properties, electrical conductivity and microstructure of copper wires processed at different cold drawing strains were studied, and the following conclusions can be drawn:

1) With increasing drawing strain, the grains were stretched along the drawing direction and gradually formed fibrous structures parallel to

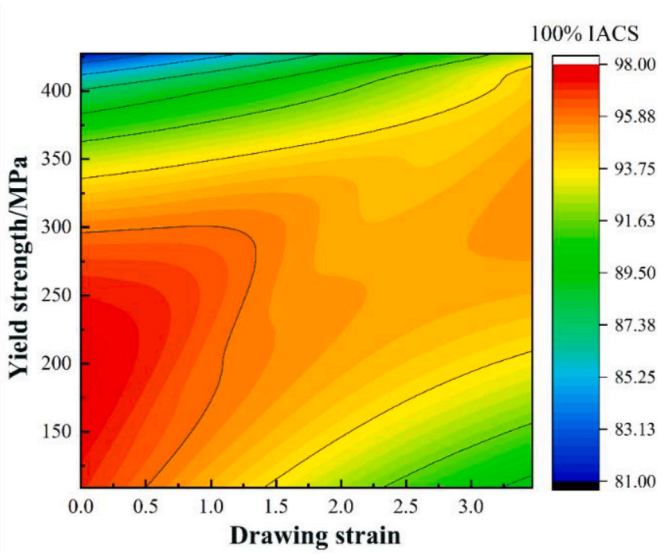

Fig. 13. Electrical conductivity versus drawing strain and yield strength.

the drawing direction. EBSD analysis showed that the grains formed two kinds of texture <001 > and <111 >. TEM results showed that with increasing strain, a large number of substructures were formed, and the dislocation density increased sharply. At the strains greater than 1.91, dynamic recrystallization took place, and the dislocation density decreased.

2) With an increase in drawing strain, the yield strength of copper wires first increased and then decreased slightly, before rising up and reaching a peak value at $\varepsilon = 1.91$, which is 427.5 MPa. The percent elongation decreased monotonously and levelled off when drawing strains went beyond 1.9.
3) The electrical conductivity of the copper wires first decreased and then increased with drawing strain. The lowest conductivity was identified to be 87.5% IACS at strain $\varepsilon = 1.91$, which was approximately 9.5% lower than that of the original copper structure. The electrical conductivity was less affected by the presence of dislocations and vacancies and was mainly compromised by the number of high-angle grain boundaries perpendicular to the drawing direction.

CRediT authorship contribution statement

Fei Yang: Executor of the experiment, Writing and Editing. **Liming Dong:** Analysis of research results. **Lei Cai:** Analysis of research results. **Linfeng Wang:** Analysis of research results. **Zonghan Xie:** Reviewing and Editing. **Feng Fang:** Designer of the experiment, Editing, Supervision.

Declaration of competing interest

The authors declare that they have no known competing financial interests or personal relationships that could have appeared to influence the work reported in this paper.

Acknowledgement

This work is supported by the Natural Science Foundation of China (grant no. 51371050), the Science and Technology Advancement Program of Jiangsu Province (BA2017112) and the 333 projects of Jiangsu Province, China (BRA2018045). The study was also partly supported by Industry-University Research Cooperation Project of Jiangsu Province, China (BY2018194).

References

[1] Q. Hu, C. Zhao, Z. Zhang, J. Guo, C. Yu, Z. Sun, X. Piao, Sonochemical synthesis of silver nanoparticles coated copper wire for low-temperature solid state bonding on silicon substrate, Chin. Chem. Lett. 30 (2019) 1455–1459.
[2] C. Zhu, A. Ma, J. Jiang, X. Li, J. Chen, Effect of ECAP combined cold working on mechanical properties and electrical conductivity of Conform-produced Cu-Mg alloys, J. Alloys Compd. 582 (2014) 135–140.
[3] L. Lu, Y. Shen, X. Chen, L. Qian, K. Lu, Ultrahigh strength and high electrical conductivity in copper, Science 304 (2004) 422–426.
[4] Y. Miyajima, S.Y. Komatsu, M. Mitsuhara, S. Hata, H. Nakashima, N. Tsuji, Change in electrical resistivity of commercial purity aluminium severely plastic deformed, Philos. Mag. A 90 (2010) 4475–4488.
[5] P.V. Andrews, M.B. West, C.R. Robeson, The effect of grain boundaries on the electrical resistivity of polycrystalline copper and aluminium, Philos. Mag. A 19 (1969) 887–898.
[6] M.C. Martin, K.F. Welton, The change in electrical resistivity with plastic deformation of aluminum and nickel, Acta Mater. 15 (1967) 571–573.
[7] Z.Y. Pan, J.B. Chen, J.F. Li, Microstructure and properties of rare earth-containing Cu–Cr–Zr alloy, Trans. Nonferrous Metals Soc. China 25 (2015) 1206–1214.
[8] M. Kulczyk, W. Pachla, J. Godek, J. Smalc-Koziorowska, J. Skiba, S. Przybysz, M. Wróblewska, M. Przybysz, Improved compromise between the electrical conductivity and hardness of the thermo-mechanically treated CuCrZr alloy, Mater. Sci. Eng. 724 (2018) 45–52.
[9] V. Spuskanyuk, O. Davydenko, A. Berezina, O. Gangalo, L. Sennikova, M. Tikhonovsky, D. Spiridonov, Effect of combining the equal-channel angular hydroextrusion, direct hydroextrusion and drawing on properties of copper wire, J. Mater. Process. Technol. 210 (2010) 1709–1715.
[10] P.P. Pal-Val, Y.N. Loginov, S.L. Demakov, A.G. Illarionov, V.D. Natsik, L.N. Pal-Val, A.A. Davydenko, A.P. Rybalko, Unusual Young's modulus behavior in ultrafine-grained and microcrystalline copper wires caused by texture changes during processing and annealing, Mater. Sci. Eng. 618 (2014) 9–15.
[11] D. Mesguich, C. Arnaud, F. Lecouturier, N. Ferreira, G. Chevallier, C. Estournès, A. Weibel, C. Josse, C. Laurent, High strength-high conductivity carbon nanotube-copper wires with bimodal grain size distribution by spark plasma sintering and wire-drawing, Scripta Mater. 137 (2017) 78–82.
[12] J.P. Hou, R. Li, Q. Wang, H.Y. Yu, Z.J. Zhang, Q.Y. Chen, H. Ma, X.M. Wu, X.W. Li, Z.F. Zhang, Three principles for preparing Al wire with high strength and high electrical conductivity, J. Mater. Sci. Technol. 35 (2019) 742–751.
[13] K. Hanazaki, N. Shigeiri, N. Tsuji, Change in microstructures and mechanical properties during deep wire drawing of copper, Mater. Sci. Eng. 527 (2010) 5699–5707.
[14] H. Park, S.H. Kim, W.J. Lee, J.W. Ha, S.J. Kim, H.J. Lee, Effect of wire-drawing process conditions on secondary recrystallization behavior during annealing in high-purity copper wires, Met. Mater. Int. (2020), https://doi.org/10.1007/s12540-020-00682-0.
[15] J. Xu, J. Li, D. Shan, B. Guo, Microstructural evolution and micro/meso-deformation behavior in pure copper processed by equal-channel angular pressing, Mater. Sci. Eng., A 664 (2016) 114–125.
[16] A.P. Zhilyaev, T.G. Langdon, Using high-pressure torsion for metal processing: fundamentals and applications, Prog. Mater. Sci. 53 (2008) 893–979.
[17] Y. Saito, H. Utsunomiya, N. Tsuji, T. Sakai, Novel ultra-high straining process for bulk materials-development of the accumulative roll-bonding (ARB) process, Acta Mater. 47 (1999) 579–583.
[18] M.Y. Murashkin, I. Sabirov, X. Sauvage, R.Z. Valiev, Nanostructured Al and Cu alloys with superior strength and electrical conductivity, J. Mater. Sci. 51 (2015) 33–49.
[19] X. Sauvage, E.V. Bobruk, M.Y. Murashkin, Y. Nasedkina, N.A. Enikeev, R.Z. Valiev, Optimization of electrical conductivity and strength combination by structure design at the nanoscale in Al–Mg–Si alloys, Acta Mater. 98 (2015) 355–366.
[20] W. Zeng, J. Xie, D. Zhou, Z. Fu, D. Zhang, E.J. Lavernia, Bulk Cu-NbC nanocomposites with high strength and high electrical conductivity, J. Alloys Compd. 745 (2018) 55–62.
[21] F. Dalla Torre, R. Lapovok, J. Sandlin, P.F. Thomson, C.H.J. Davies, E.V. Pereloma, Microstructures and properties of copper processed by equal channel angular extrusion for 1–16 passes, Acta Mater. 52 (2004) 4819–4832.
[22] Z.S. Niewczas, J.D. Basinski, M. Emb, Deformation of copper single crystals to large strains at 4 2K - II. Transmission electron. microscopy observations of defect structure, Philos. Mag. A 81 (2001) 1143–1159.
[23] D.A. Hughes, N. Hansen, Microstructure and strength of nickel at large strains, Acta Mater. 48 (2000) 2985–3004.
[24] N. Guo, D. Li, H. Yu, R. Xin, Z. Zhang, X. Li, C. Liu, B. Song, L. Chai, Annealing behavior of gradient structured copper and its effect on mechanical properties, Mater. Sci. Eng. 702 (2017) 331–342.
[25] J.A. Muñoz, O.F. Higuera, J.A. Benito, D. Bradai, T. Khelfa, R.E. Bolmaro, A. M. Jorge, J.M. Cabrera, Analysis of the micro and substructural evolution during severe plastic deformation of ARMCO iron and consequences in mechanical properties, Mater. Sci. Eng. 740–741 (2019) 108–120.
[26] X.B. Li, G.M. Jiang, J.P. Di, Y. Yang, C.L. Wang, Effect of cryogenic rolling on the microstructural evolution and mechanical properties of pure copper sheet, Mater. Sci. Eng. 772 (2020) 138811.
[27] Y.S. Li, N.R. Tao, K. Lu, Microstructural evolution and nanostructure formation in copper during dynamic plastic deformation at cryogenic temperatures, Acta Mater. 56 (2008) 230–241.
[28] J.J. Wang, N.R. Tao, K. Lu, Revealing the deformation mechanisms of nanograins in gradient nanostructured Cu and CuAl alloys under tension, Acta Mater. 180 (2019) 231–242.
[29] L.S. Toth, C. Gu, Ultrafine-grain metals by severe plastic deformation, Mater. Char. 92 (2014) 1–14.
[30] J.P. Hou, R. Li, Q. Wang, H.Y. Yu, Z.J. Zhang, Q.Y. Chen, H. Ma, X.M. Wu, X.W. Li, Z.F. Zhang, Breaking the trade-off relation of strength and electrical conductivity in pure Al wire by controlling texture and grain boundary, J. Alloys Compd. 769 (2018) 96–109.
[31] N.K. Kumar, B. Roy, J. Das, Effect of twin spacing, dislocation density and crystallite size on the strength of nanostructured α-brass, J. Alloys Compd. 618 (2015) 139–145.
[32] S.M. Dasharath, C.C. Koch, S. Mula, Effect of stacking fault energy on mechanical properties and strengthening mechanisms of brasses processed by cryorolling, Mater. Char. 110 (2015) 14–24.
[33] R.W. Armstrong, W.L. Elban, Crystal strengths at micro- and nano-scale dimensions, Cryst 10 (2020) 88.
[34] J. Grum, Book review: mechanical behavior of materials by M.A. Meyers and K.K. Chawla, Int. J. Microstruct. Mater. Prop. 4 (2009) 686.
[35] F. Yang, L. Dong, X. Hu, X. Zhou, Z. Xie, F. Fang, Effect of solution treatment temperature upon the microstructure and mechanical properties of hot rolled Inconel 625 alloy, J. Mater. Sci. 55 (2020) 5613–5626.
[36] N. Hansen, Boundary strengthening in undeformed and deformed polycrystals, Mater. Sci. Eng. 409 (2005) 39–45.
[37] P. Rodríguez-Calvillo, N. Ferrer, J.M. Cabrera, Analysis of microstructure and strengthening in CuMg alloys deformed by equal channel angular pressing, J. Alloys Compd. 626 (2015) 340–348.
[38] J. Gubicza, N.Q. Chinh, J.L. Lábár, S. Dobatkin, Z. Heged S, T.G. Langdon, Correlation between microstructure and mechanical properties of severely deformed metals, J. Alloys Compd. 483 (2009) 271–274.

[39] X. Ma, J. Chen, X. Wang, Y. Xu, Y. Xue, Microstructure and mechanical properties of cold drawing CoCrFeMnNi high entropy alloy, J. Alloys Compd. 795 (2019) 45–53.
[40] G.D. Sathiaraj, A. Pukenas, W. Skrotzki, Texture formation in face-centered cubic high-entropy alloys, J. Alloys Compd. 826 (2020) 154183.
[41] D.N. Lee, Y.H. Chung, M.C. Shin, Preferred orientation in extruded aluminum-alloy rod, Scripta Mater. 17 (1983) 339–342.
[42] A.A. Luhvich, A.S. Karolik, Calculation of electrical resistivity produced by dislocations and grain boundaries in metals, J. Phys. Condens. Matter 6 (1994) 872.
[43] A. Matthiessen, C. Vogt, On the influence of temperature on the electric conducting-power of alloys, Proc. Roy. Soc. Lond. 12 (1862) 1–27.
[44] Z.S. Basinski, J.S. Dugdale, A. Howie, The electrical resistivity of dislocations, Philos. Mag. A 8 (1963) 1989–1997.
[45] L.H. Qian, Q.H. Lu, W.J. Kong, K. Lu, Electrical resistivity of fully-relaxed grain boundaries in nanocrystalline Cu, Scripta Mater. 50 (2004) 1407–1411.
[46] D. Setman, E. Schafler, E. Korznikova, M.J. Zehetbauer, The presence and nature of vacancy type defects in nanometals detained by severe plastic deformation, Mater. Sci. Eng. 493 (2008) 116–122.
[47] H. Pan, Y. He, X. Zhang, Interactions between dislocations and boundaries during deformation, Materials 14 (2021) 1012–1060.